Creation Research Society Quarterly 2015. 51:248–258.

Soft Bone Material from a Brow Horn of a *Triceratops horridus* from Hell Creek Formation, Montana

Mark Armitage

Abstract

Soft fibrillar bone tissues were discovered within a brow horn of *Triceratops horridus* collected at the Hell Creek Formation in Montana. Soft material was present in pre- and post-decalcified bone. Horn material yielded numerous small sheets of bone matrix that had yet to turn into hard bone. This matrix possessed visible structures consistent with bone osteocytes. Some sheets of soft tissue had multiple layers of intact osteocyte tissues featuring elegant filipodial interconnections and secondary branching. Both oblate and stellate types of osteocyte-like cells were present in sheets of soft tissues. SEM analysis yielded osteocyte cells featuring filipodial extensions of 18 to 20 microns in length. Filipodial extensions were delicate and showed no evidence of any permineralization or crystallization artifact and therefore were interpreted to be soft. This work is the first to report soft tissues from adult *Triceratops* horn in a Creation journal.

Introduction

Many studies have reported the presence of soft tissues and cells in what were thought to be fossilized dinosaur bones from many taxa, including *Tarbosaurus bataar*, *Tyrannosaurus rex*, *Brachylophosaurus canadensis*, and *Triceratops horridus* (Pawlicki, 1978; Pawlicki and Nowogrodzka-Zagorska, 1998; Schweitzer and Horner, 1999; Armitage, 2001; Zylberberg and Laurin, 2011), as well as other extinct organisms such as certain marine turtles (Cadena and Schweitzer, 2012).

Studies using light and electron microscopy have identified tissue components of dinosaur remains, such as red blood cells, endothelial cells, osteocytes, and collagen fibers (Schweitzer et al. 2005, 2007a, 2009). Additionally, molecular peptides and proteins also have been identified and have helped to confirm the cellular nature of these fine structures (Schweitzer et al., 2007b, 2009; Lindgren et al., 2011; San Antonio et al., 2011).

Critiques of these findings have been mounted by Kaye et al. (2008), who contend that these soft remains are merely the leftover biofilms of microbial activity on decaying tissues; however recent analyses seem to confirm that original soft tissues and possibly original molecules do exist in incompletely fossilized remains of extinct animals, including dinosaurs (Schweitzer et al.,

Accepted for publication March 20, 2015

2009; Lindgren et al., 2011; Cadena and Schweitzer, 2012; Schweitzer et al., 2013).

Furthermore, a large variety of specimens yielding soft tissues supports the fact that soft tissue is not limited to known fossil sites or fossil species. Therefore, recent work has focused on sampling fossils from various types of ancient organisms (dinosaur and otherwise), depositional environments, and geologic time frames to determine the extent of soft tissue presence in Devonian, Triassic, and Cretaceous layers. Comparisons have then been made with recently excavated specimens (Schweitzer et al., 2007a; Zylberberg and Laurin, 2011).

The purpose of this study was to perform microscopy on fresh fossil specimens of *Triceratops* brow horn and ribs for the presence of soft tissues and to characterize any soft tissues found.

Materials and Methods

An intact *Triceratops* horn (HCTH-00) was recovered on May 12, 2012, from a well-sorted, water-buried sandstone within the Hell Creek Formation at a previously unexcavated site in Glendive, Montana. The recovered horn was uncovered, protected with casting materials, and removed. The size and external morphology of the fossil was consistent with other *Triceratops* horns recovered from the Hell Creek Formation.

Disarticulated *Triceratops* ribs (HCTR-11) and vertebrae (HCTV-22) found within a mile of the horn also were recovered for analysis.

In the laboratory, hand-sized pieces of HCTH-00 were fixed in 2.5% glutaraldehyde, buffered with 0.1M sodium cacodylate buffer, rinsed in distilled water and buffer, and stored in PBS. Individual pieces of roughly 20 cm^2 were removed by pressure fracture (HCTH-01, 02, 03) and examined under a dissecting microscope to identify and collect soft material.

Soft materials recovered were washed in pure water and stored in PBS to await further analysis. Other horn specimens (HCTH-04, 05) were processed through a decalcification protocol.

Several pieces about 20 to 50 cm in size were rinsed in water after fixation and were placed into a solution of 14% sodium EDTA at room temperature. EDTA was exchanged every two to four days for a period of four weeks. Significant bone mineral remained after 4 weeks; therefore, some pieces were left in decalcification solution for a period of two months. Complete decalcification never took place; that is, some large fragments of horn remained after two months of soaking, so it is unknown if longer-term soaking would yield soft and transparent, vessel-like tissues such as previously reported (Schweitzer, et al., 2005, 2007a, 2007b, 2009; Lindgren et al., 2011).

Decalcified bone pieces were air-dried, glued to aluminum stubs, sputter coated with gold for 60 seconds at 20mA, and imaged at 20kV on a Hitachi S2500 scanning electron microscope (SEM).

Large strips of thin, light brown, soft material (20cm by 10cm) were recovered from innermost interior sections of other fixed and unfixed, non-decalcified horn bone pieces. Strips were postfixed in 2% osmium tetroxide, dehydrated in a graded series of acetone, and infiltrated with a polymer resin (EMBed-812, Electron Microscopy Sciences, Ft. Washington, PA).

Other strips of soft material were cut into 2cm by 2mm pieces, embedded in OCT (Sakura Tissue Tek, Japan) and sectioned on a Microm (Thermo Scientific) HM550 cryostat at -23C. Cryosections of 9–11 micron thickness were affixed to glass slides, and coverslipped for light microscopy. Photo documentation was performed using a Jenoptik (Jena, Germany) C14+ camera on a Nikon 80i microscope.

Triceratops rib specimens were allowed to air-dry and were subsequently fractured with mechanical pressure yielding 5–10mm-sized pieces suitable for SEM. Pieces of rib with their internal surfaces exposed were sputter-coated and examined with SEM.

Picrosirius stain was employed for the presence of collagen; however, results were inconclusive.

Figure 1. *Triceratops* supraorbital horn specimen, in matrix prior to coating in methylmethacrylate, Hell Creek Formation, Glendive, MT.

Results

A fragment of the *Triceratops* horn (Figure 1) approximately 100 cm long, 22 cm in diameter, and 9 kg in mass was obtained for analysis. The outer sheath of keratin was not found. The horn had been partially buried under 30 cm of homogeneous but loosely packed sandstone and rock. The rock required fracturing by hammer and chisel to free the distal part of the horn. Rib fragments (Figure 2), located separately from the horn, were approximately 15 cm long and had no visible moisture when removed.

Horn material was not completely desiccated but appeared somewhat moist during excavation (Figure 3). Soft, moist, muddy material could be seen surrounding pores of bone vessels on inner horn surfaces (Figure 4).

After removal, the horn fractured into several large pieces (Figures 3, 4). Individual large pieces were wrapped separately in aluminum foil, sealed in containers and transported to the lab for analysis.

Fixed horn material did not seem as friable as unfixed material, possibly because interior soft tissues were stabilized by fixatives. Small (2–5 mm) red and brown plant roots were loosely attached to exterior surfaces and extended into fractures in the horn (see left side of bone in Figure 4).

Pieces of small, fixed material from the inner core of the horn came apart with moderate hand pressure and were found to contain thin, elastic, reddish-brown flaps of soft material (Figure 5, black arrow), which could be peeled away from the bone in sheets and stretched to almost double the original size.

It was initially thought that this soft material might represent the remains of a biofilm and/or plant material due to the many tiny plant roots associated with it (Figure 6, black arrows). These reddish-brown flaps of soft material and the off-white to milky-white pieces of soft material (Figure 7, white arrows) collected from pre- and post-decalcified bones yielded innumerable small sheets of unmineralized bone matrix with clearly visible cells consistent with lacunar bone osteocytes. Osteocytes also exhibited internal structures consistent with cellular organelles (Figures 9–10, arrows).

Figure 2. *Triceratops* rib specimen, pre-extraction, Hell Creek Formation, MT.

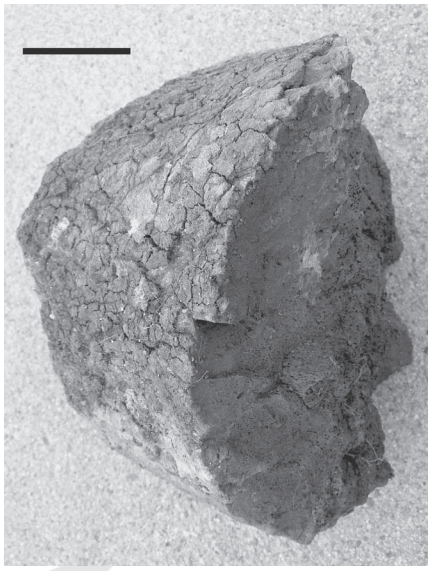

Figure 3. *Triceratops* supraorbital horn, 20 cm by 20 cm unfixed specimen. Scale bar = 2.5 cm.

Figure 4. Close-up of bottom surface of horn from Figure 3. Note porosity of vascular channels in horn bone. Scale bar = 1.8 cm.

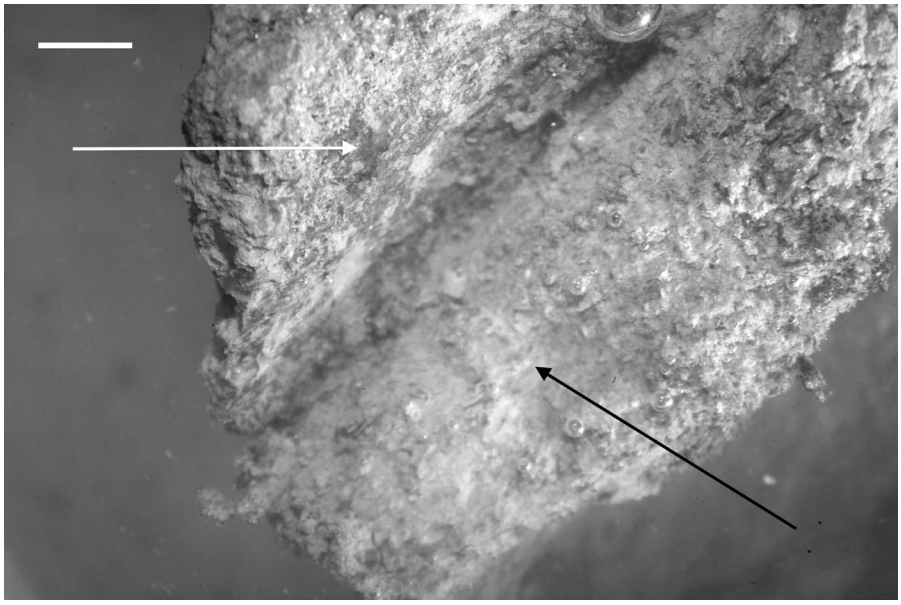

Figure 5. Light micrograph, flap of fixed soft tissue (black arrow) slightly peeled away from undecalcified *Triceratops* bone specimen (white arrow), 10X magnification. Scale bar = 0.75 mm.

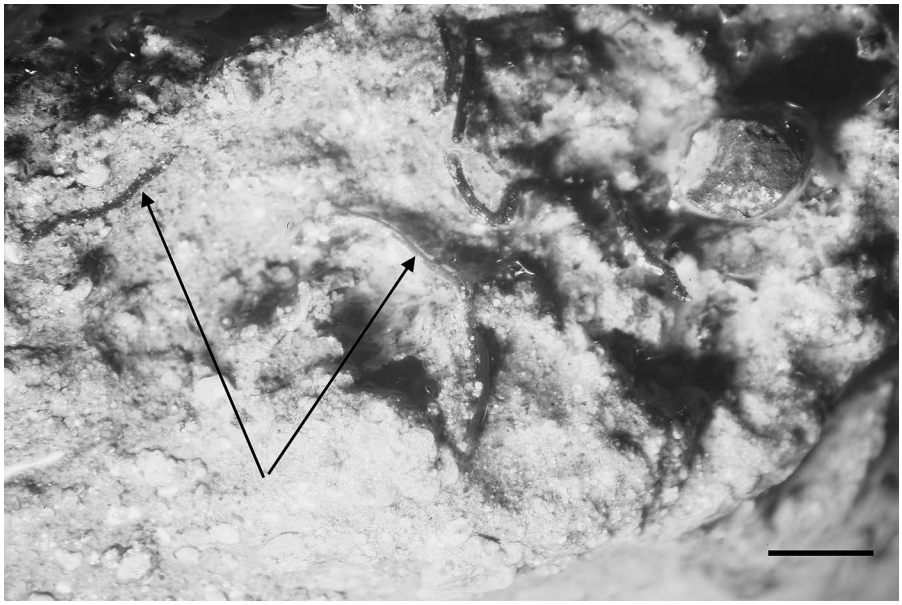

Figure 6. Light micrograph, underside of soft tissue from Figure 5. Note slender, curved plant rootlets (black arrows). Scale bar = 0.5 mm.

The matrix of soft bone densely populated with osteocytes (Figures 8–10) was identical to osteocytes found in compact bone of *Tyrannosaurus rex* femur (Schweitzer et al., 2005, 2013), *Brachylophosaurus canadensis* femur (Schweitzer et al., 2009), and *Prognathodon* sp. femur (Lindgren et al., 2011).

Flexible vessels were not present, and demineralization over two months did not completely dissolve the bone mineral; therefore it was halted. Both processed and unprocessed horn specimens exhibited many clear to milky-white or reddish brown pieces of soft material, which swayed gently upon bone surfaces when solutions were disturbed.

Soft material processed for polymer thin sectioning disintegrated during sectioning, possibly because of a negative effect of the dehydration or maybe because of incomplete infiltration.

Fractured rib specimens contained well-preserved Haversian systems, with many visible lamellae and lacunae (Figure 11). The Haversian canals sometimes were filled with many spherical objects (Figure 12), which are consistent with the size and shape of red blood cells (RBCs). So many RBCs were present that vessel structure was often obscured.

Many soft, hollow, cylindrical tubes were seen to project from Haversian canals (Figure 13) and are consistent with the size and shape of blood vessels.

Non-decalcified horn specimens showed good preservation of mineralized vessel structures surrounded by dense cortical bone. Decalcified horn specimens also were characterized by vessels present in vertical conformation (as they would be in Haversian canals), and interconnecting Volkmann's canals are evident (white arrows, Figure 14), yet all vessel-like structures studied were fully permineralized.

A fractured end of a vessel in Figure 15 (white arrow) is further magnified in Figure 16, and it is clear that microstructures within it (possibly blood and lymph) are also fully permineralized. It therefore appeared that permineralization was selective or, at the least, that some soft tissues were sequestered from the process of fossilization. Further study of the horn must be done to determine if

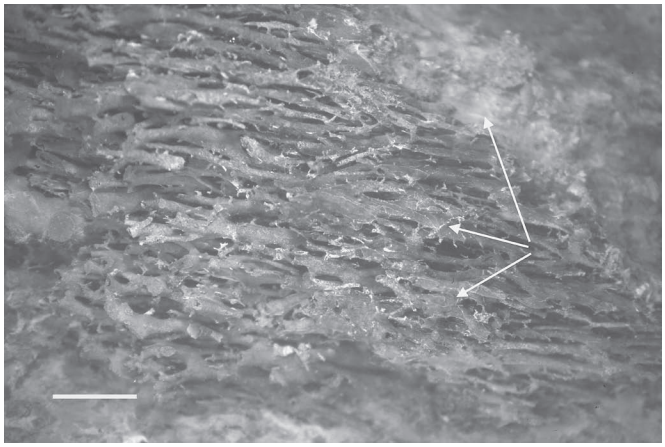

Figure 7. Light micrograph of decalcified portion of *Triceratops* horn bone, 20X magnification. Note white portions of unfossilized, soft tissues that adhere to permineralized vessel elements (arrows). Scale bar = 0.5 mm.

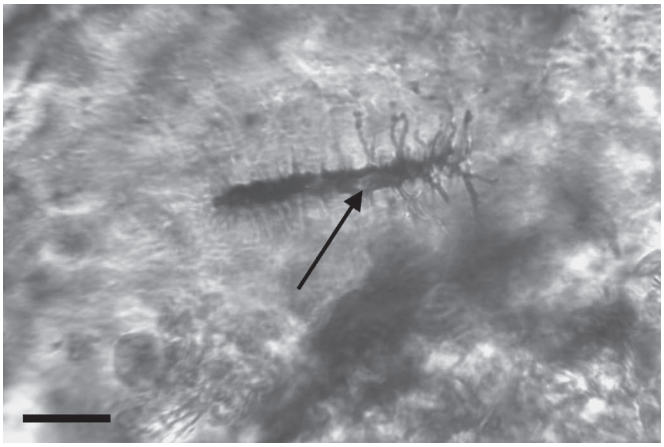

Figure 9. Light micrograph of a section from a sheet of soft, fibrillar bone material from un-decalcified *Triceratops* horn, magnification 1100X. Note intracellular organelle-like structures (arrow). Scale bar = 50 microns.

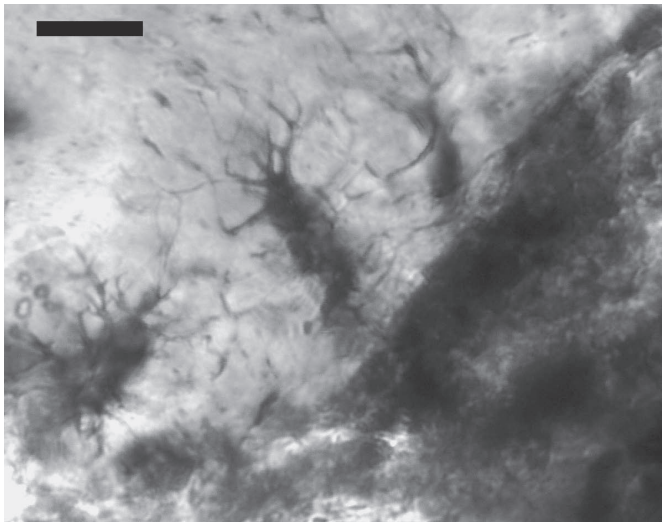

Figure 8. Light micrograph of a section from a sheet of soft, fibrillar bone material from un-decalcified *Triceratops* horn, magnification 800X. Note three osteocytes with fine filopodial processes that interconnect (lower right). Scale bar = 50 microns.

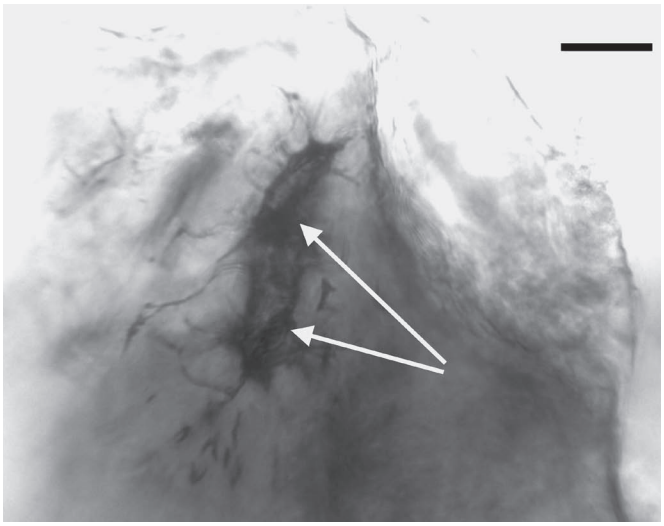

Figure 10. Light micrograph of a section from a sheet of soft, fibrillar bone material from un-decalcified *Triceratops* horn. Note intracellular organelle-like structures (arrows).

this seemingly selective permineralization is related to anatomical differences within the horncore (Happ, 2010).

SEM analysis of decalcified portions of horn shows a large number of osteocytes with very fine filipodial projections lying along the same layer of fibrillar bone (Figures 17–19).

Aliquots of post-decalcification EDTA pipetted onto glass slides were observed to contain individual osteocytes; therefore, small volumes of decalcification solutions collected from the bottom surface of decalcification jars were dialyzed in pure water over several changes, and washed cells were isolated on heat-fixed slides (Figures 20–21).

Discussion

The Hell Creek Formation is a well-characterized and studied rock unit that was first described in the early 1900s (Brown, 1907). It is exposed by the well-known Cedar Creek Anticline at Glendive, Montana and encompasses nearly 700km (Johnson

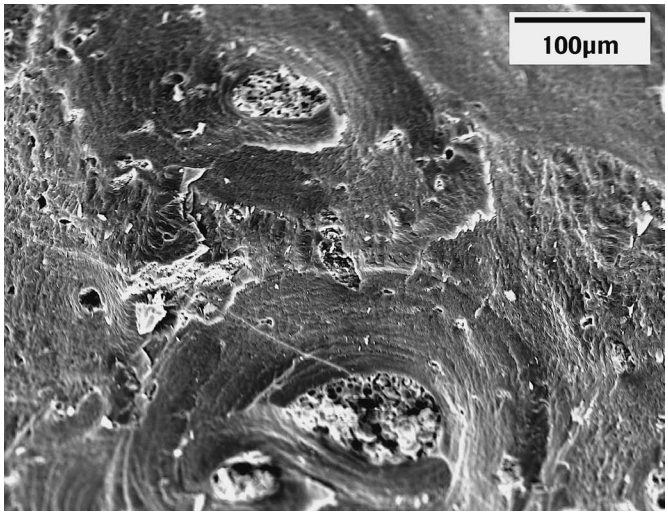

Figure 11. Scanning electron micrograph (SEM) of compact fractured bone material from un-decalcified *Triceratops* rib, magnification 120X. Note well-defined circular Haversian system. Also note that the center of each Haversian system is populated by possible preserved blood products.

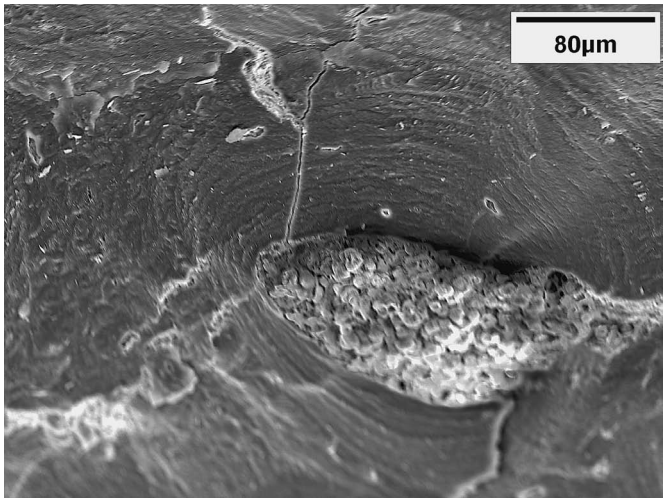

Figure 12. SEM of compact fractured bone material from un-decalcified *Triceratops* rib, magnification 300X. Note well-defined circular Haversian system populated at the center with possible preserved blood products and red blood cell-like microstructures.

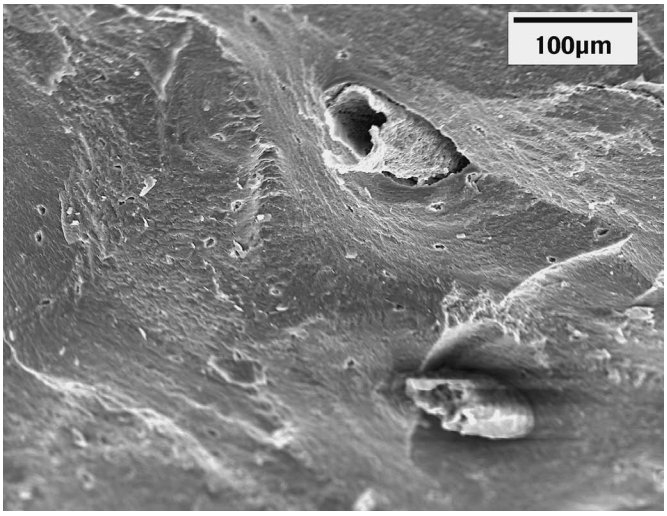

Figure 13. SEM of compact fractured bone material from un-decalcified *Triceratops* rib, magnification 350X. Note hollow blood vessel emanating from Haversian canal. Blood vessels are flexible and pliable.

et al., 2002). Many valuable fossils have been recovered from the Hell Creek Formation exposed at Glendive, and *Triceratops* remains (including brow horns) are frequently found at that location (Horner, 2001).

This work represents the first to report soft tissues from a *Triceratops* horn (Armitage and Anderson, 2013). This offers a unique opportunity to understand horn form and function. *Triceratops* horn anatomy has been rarely studied, thus much remains to be known about their structure.

Anatomically, *Triceratops* horn offers a unique fossil structure with differentiated inner layers of varying thickness and porosity. Below the keratin sheath (altered and mineralized by the fossilization process) lies an outer bone layer (OBN) of approximately 1–5 mm thickness, composed of compact Haversian bone that is deeply embedded with vascular tissues (Happ, 2010). Within the OBN is the horncore made up of highly vascularized trabecular bone. The trabecular horncore extends almost the entire length of the horn but terminates into a cornusal sinus at the base of the horn where it joins the skull.

Triceratops fossils are considered common within the Hell Creek Formation (Happ, 2010). Discovery of soft tissue in *Triceratops* horn provides additional insight into the nature of fossilization and extends our understanding on the prevalence of preserved original dinosaur tissue.

No tissues or vessels floated away from bones in solution. As described, however, solutions were examined post-decalcification for the presence of free-floating osteocytes, and they were successfully isolated. It is hoped that planned immunohistochemistry experiments will detect endogenous proteins.

Decalcification was performed for 20 weeks, which would have seemed sufficient time to expose soft tissues for collection, but bone mineral was never fully dissolved, so it is unknown if soft vessels would have remained had decalcification been carried out longer. Further study is required to determine if

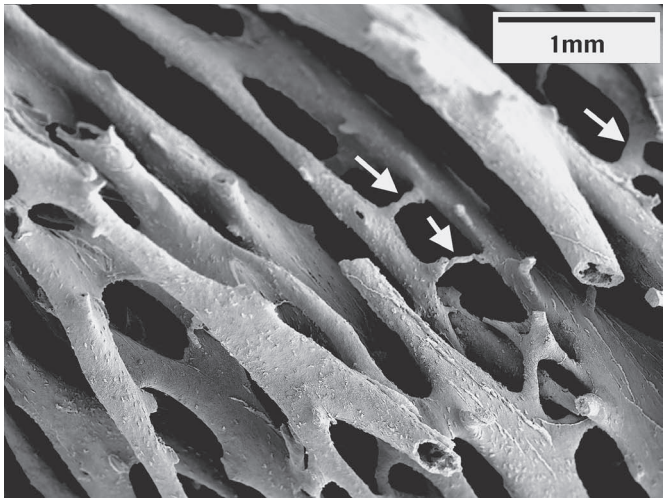

Figure 14. SEM of decalcified bone material from highly vascular portion of *Triceratops* horn, magnification 25X. All of the bone mineral has been dissolved away, leaving intact permineralized vessels. Volkmann's canals link Haversian canal vessels together (white arrows).

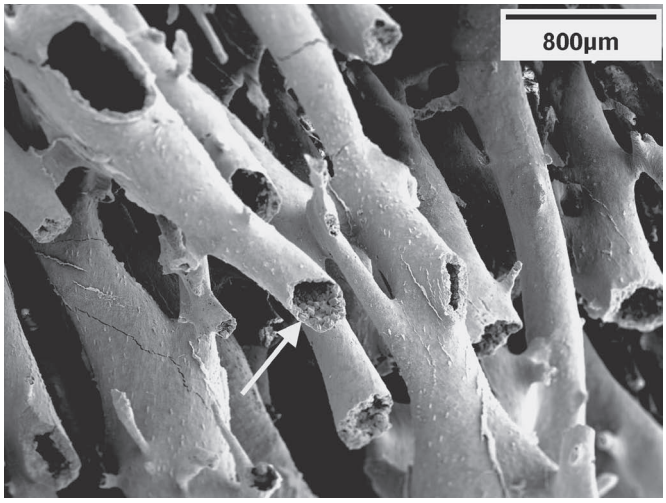

Figure 15. SEM close-up similar to Figure 14. Magnification 30X. Note possible blood products lining inner wall of hardened vessel (white arrow).

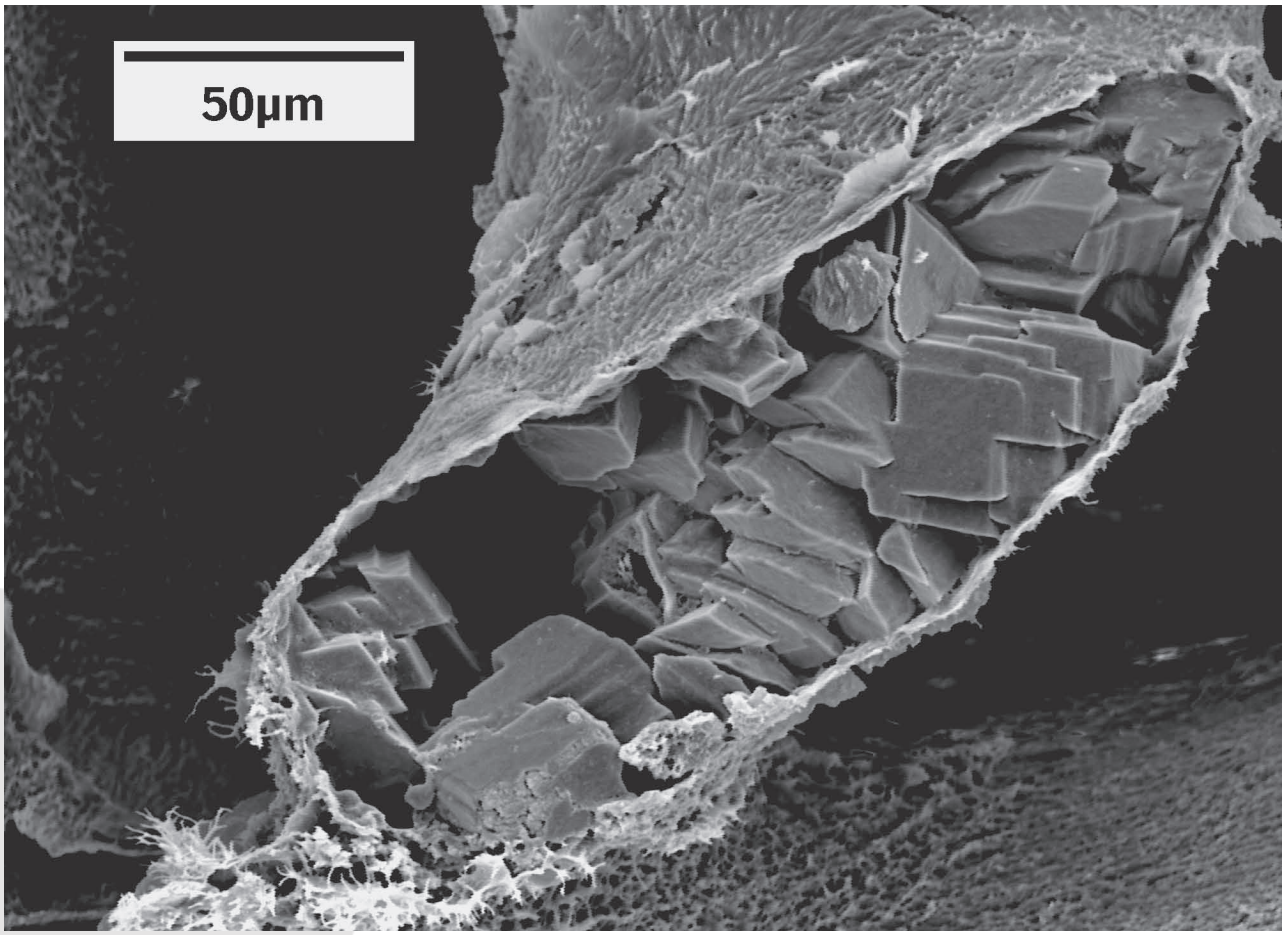

Figure 16. SEM close-up from another vessel. Magnification 200X. Note crystallized nature of possible blood products lining inner wall of hardened vessel.

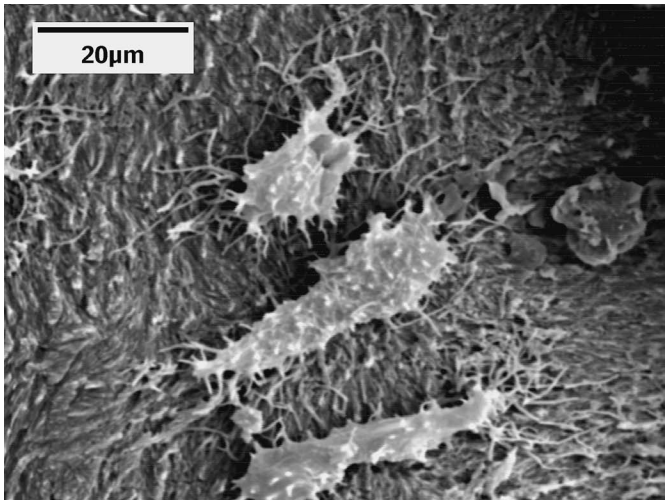

Figure 17. SEM of decalcified bone material from *Triceratops* horn, magnification 200X. Note two large oblate osteocytes lying on fibrillar bone matrix.

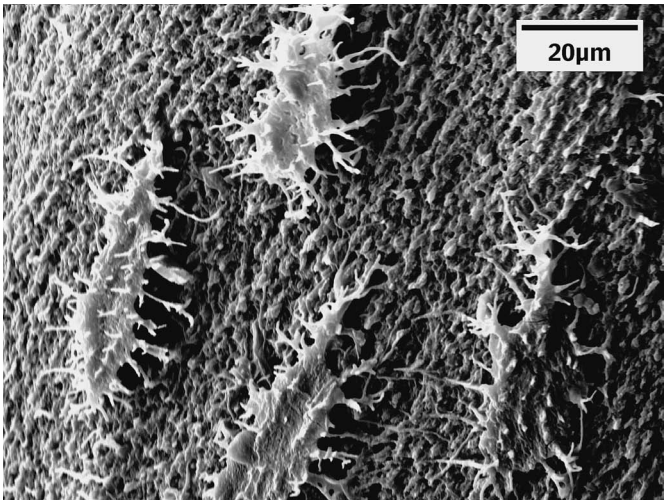

Figure 19. SEM of decalcified bone material from *Triceratops* horn, magnification 1000X. Note four osteocytes lying on fibrillar bone matrix. Cell filipodia are anchored into the bone matrix and have diameters approaching 200nm.

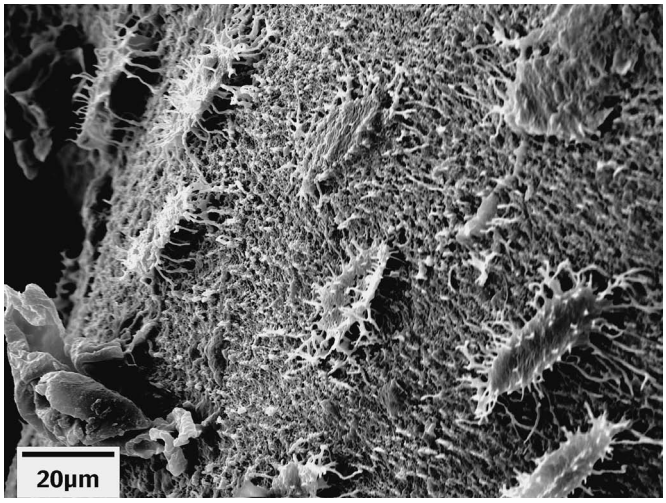

Figure 18. SEM of decalcified bone material from *Triceratops* horn, magnification 600X. Note oblate osteocytes lying on fibrillar bone matrix. Tiny white filipodial processes from cells beneath the layer can be seen extruding through.

intact, soft vessels might be recovered from completely demineralized horn specimens.

Kaye et al. (2008) maintain that the soft tissue from dinosaur fossils is polysaccharide from a microbial biofilm. They suggest that the polysaccharide film forms a cast of the tissue while bacteria are decomposing organic remains (soft bone tissues). Once dissolved from the fossilized bone matrix, this film purportedly retains the shape of vessels and osteocytes. They conclude that what has been described as intact tissue is actually biofilm polysaccharide.

Moreover, Rasmussen et al. (2003) report that some microorganisms can form collagen-like proteins, which Kaye et al. (2008) suggest might be mistaken for dinosaur collagen.

However, Kaye et al. (2008) are not clear regarding the mechanism by which microbes might replicate stellate and oblate osteocytes (Cadena and Schweitzer, 2012) in such well-preserved and fine detail; including internal nucleus-like spheres, primary and secondary filipodia, and cell-to-cell junctions, such as those reported in this paper.

If such a microbial replication mechanism were discovered, it could eclipse the exquisite siliceous production and assembly systems employed by diatom cells to create the compelling geometric valves known by microscopists the world over (Sumper and Bruner, 2006; Tesson and Hillebrand, 2010). Sophisticated replication systems used by diatoms are very poorly understood, but to uncover the method by which a bacterial biofilm could replicate the very cells the bacteria are decomposing would be astonishing.

In addition, it is not clear how such biofilm structures could themselves survive the ravages of time. Once produced, other microorganisms could begin to digest these initial biofilms. Such biofilm regeneration over time would not be consistent with the retention of the cellular detail reported here and by others.

Bone material examined in this study was found undesiccated; therefore, microbial activity could have been supported

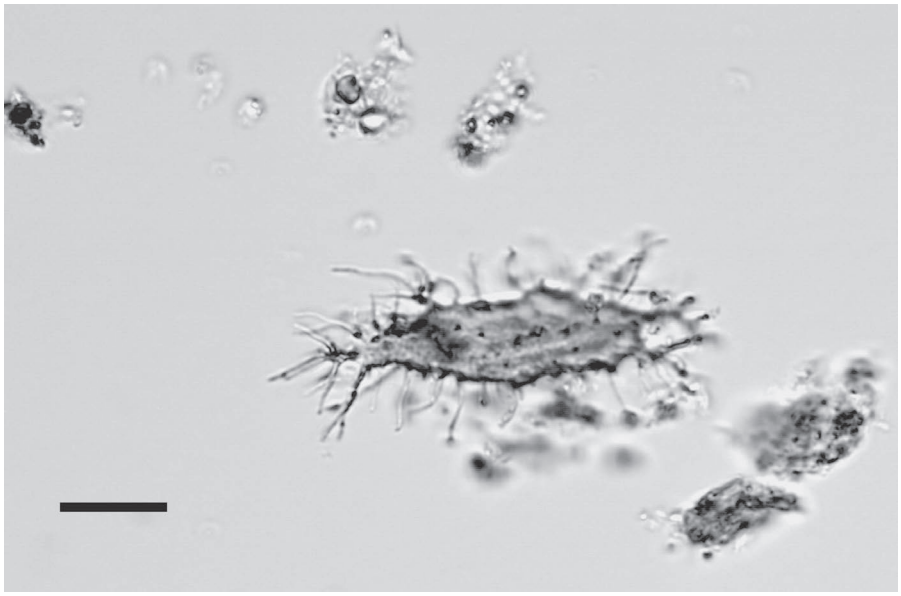

Figure 20. Light micrograph of individual isolated osteocyte on a glass slide.

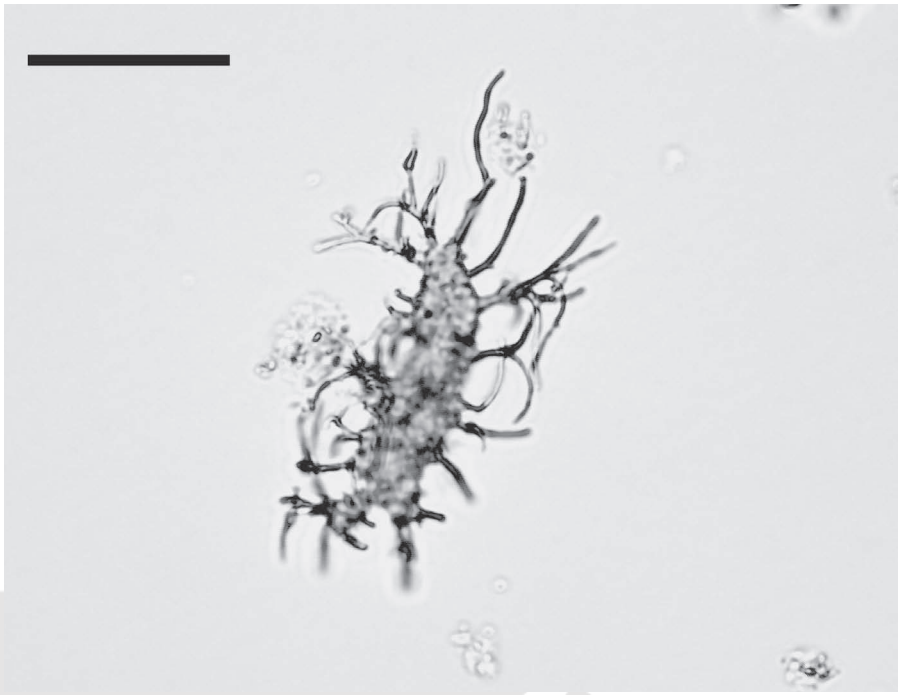

Figure 21. Higher magnification light micrograph of a single decalcified osteocyte.

within this specimen after burial.

The most parsimonious explanation is that these are original tissues, not highly reproducible organic ghost images of original tissues.

The fact that any soft tissues were present in this heavily fossilized horn specimen would suggest a selective fossilization process, or a sequestration of certain deep tissues as a result of the deep mineralization of the outer dinosaur bone, as described by Schweitzer et al. (2007a).

As mentioned previously, however, the horn was not desiccated when recovered and actually had a muddy matrix deeply embedded within it, which became evident when the horn fractured.

Additionally, in the selected pieces of this horn that were processed, soft tissues seemed to be restricted to narrow slivers or voids within the highly vascular bone, but further work is needed to fully characterize those portions of the horn that contained soft material.

It is unclear why these narrow areas resisted permineralization and retained a soft and pliable nature. Nevertheless, it is apparent that certain areas of the horn were only lightly impacted by the degradation that accompanied infiltration by matrix and microbial activity.

Proposing that these elastic sheets of reddish-brown soft tissues are microbial biofilm structures is not consistent with our observations of fine structure of osteocyte filipodia and their internal microstructures resembling cellular organelles (Figures 9–10).

Nevertheless the question remains: How could microbes have replicated the fine detail visible in these structures?

In addition, the filipodial processes show no evidence of crystallization, as do the fractured vessels in Figure 16, and some filipodial processes taper elegantly to 300nm widths and smaller (Figure 19).

Furthermore, if biofilms represent the sole component of these soft tissues, as suggested by Kaye et al. (2008), why are they found only within compact bone? Certainly there would seem to be sufficient nutrients in the matrix surrounding buried bones to support the production of additional biofilms. Moreover, why are the decaying roots that no longer support plant functions not covered over or completely replicated themselves by biofilms? Finally, biofilm production must have

taken place within years or decades after burial in order to capitalize on nutrients available in their original form and to faithfully replicate ultrastructure before autolysis. It does not seem reasonable to suggest the original tissues would not survive through deep time but replicated structures captured in biofilms would.

We believe it significant that large, intact sheets of dinosaur fibrillar bone matrix seemed to be more densely populated (in the z-axis) with osteocytes than in previous studies of dinosaur material (Figure 8). It also was interesting that *Triceratops* soft tissues (particularly those containing multiple layers of osteocytes) did not require staining for light microscopy.

Osteocytes normally display very fine structure, including nucleus-like spheres and secondary branching of filipodia in freshly sectioned material. We observed these nucleus-like spheres and secondary branching of filopodia.

Similarly, many transparent osteocytes and nucleus-like structures were observed in the *T. rex* material examined by Schweitzer et al. (2005, 2007b, 2013). We also observed transparent tissue structures. Initially it was thought that simply empty lacunae were being imaged; however, SEM analysis verified the presence of oblate and stellate osteocytes (Cadena and Schweitzer, 2012) with very fine structural details (to within 300nm or less). Some filipodial extensions in this study reached 18–20 microns in length, almost twice the length of those previously reported (Figures 18–19). Therefore our data is fully consistent with previous reports, and this extensive detail further complicates a biofilm explanation.

Contrary to Kaye et al. (2008), who claimed that these structures are the remains of bacterial biofilms, the vessel-like structures emanating from many of the vascular canal walls were thick, fully cylindrical, and had undulating wall surfaces consistent with extant vessel tissues (Figures 13, 16).

Furthermore, the thin strips of soft material and the vessel-like structures we discovered extended deep into the bone, which is uncharacteristic of superficial biofilms.

Schweitzer et al. (2005, 2007a, 2007b, 2009) and Asara et al. (2007) analyzed different dinosaur fossils and observed osteocytes with original transparency, extensive filipodia, and internal contents (such as a defined nuclei) within the osteocytes. As noted, this is inconsistent with the suggestion that the observed osteocytes are actually biofilm imprints mimicking the morphology of octeocytes. Such imprints would not have defined nuclei or other internal cell structures. In addition, antibodies for avian collagen I exhibited an affinity for collagen isolated from *T. rex* fossils, and this collagen was degraded by modern collagenase (Schweitzer et al., 2005).

Antibodies with an affinity for both avian and reptilian proteins also had affinity for *B. canadensis* (Schweitzer et al., 2009). Bern et al. (2009) further analyzed the specimens used by Asara et al. (2007) and confirmed the presence of an avian-like collagen with no indication of microbial collagen-like proteins. Moreover, Schweitzer et al. (2013) have detected the affinity of an avian collagen-specific antibody and a DNA-specific antibody for molecules in the tissue samples. Such affinity is indicative of the presence of avian collagen and nucleic acids in the dinosaur tissue.

Cumulatively, these characteristics are consistent with the presence of intact tissue and inconsistent with the putative presence of microbial biofilm material. Thus, it is also concluded that these data are fully consistent with the detection of intact cells and tissues that have been preserved in these *Triceratops* fossils.

References

Armitage, M. 2001. Scanning electron microscope study of mummified collagen fibers in fossil *Tyrannosaurus rex* bone. *Creation Research Society Quarterly* 38:61–66.

Armitage, M.H., and K.L. Anderson. 2013. Soft sheets of fibrillar bone from a fossil of the supraorbital horn of the dinosaur *Triceratops horridus*. *Acta Histochemica* 115(6): 603–608.

Asara, J.M., M.H. Schweitzer, L.M. Freimark, M. Phillips, and L.C. Cantley. 2007. Protein sequences from Mastodon and *Tyrannosaurus rex* revealed by mass spectrometry. *Science* 316: 280–285.

Bern, M., B.S. Phinney, and D. Goldberg. 2009. Reanalysis of *Tyrannosaurus rex* mass spectra. *Journal of Proteome Research* 8:4328–4332.

Brown, B. 1907. The Hell Creek beds of the Upper Cretaceous of Montana. *Bulletin of the American Museum of Natural History* 23:823–845.

Cadena, E.A., and M.H. Schweitzer. 2012. Variation in osteocytes morphology vs bone type in turtle shell and their exceptional preservation from the Jurassic to the present. *Bone* 51:614–620.

Happ, J.W. 2010. New evidence regarding the structure and function of the horns in *Triceratops* (Dinosauris: Caratopsidae). In Ryan, M.J., B.J. Chinnery-Allgeier, and D.A. Eberth (editors), *New Perspectives on Horned Dinosaurs*, pp. 271–281. Indiana University Press, Bloomington and Indianapolis, IN.

Horner, J. 2001. *Dinosaurs under the Big Sky*. Mountain Press Publishing Company, Missoula, MT.

Johnson , K.R., D.J. Nichols, and J.H. Hartman. 2002. Hell Creek Formation: a 2001 synthesis. In Hartman, J.H., K.R. Johnson, and D.J. Nichols (editors), *The Hell Creek Formation and the Cretaceous-Tertiary boundary in the northern Great Plains: An integrated continental record of the end of the Cretaceous*, pp. 503–510. Geological Society of America Special Paper 361, Boulder, CO.

Kaye, T.G., G. Gaugler, and Z. Sawlowicz. 2008. Dinosaur soft tissues interpreted as bacterial biofilms. *PLoS One* 3(7): e1–7.

Lindgren, J., P. Uvdal, A. Engdahl, A.H. Lee, C. Alwmark, K.E. Bergquist, E. Nils-

son, P. Ekstrom, M. Rasmussen, D.A. Douglas, M.J. Polcyn, and L.L. Jacobs. 2011. Microspectroscopic evidence of Cretaceous bone proteins. *Plos One* 6(4): e1–11.

Pawlicki, R. 1978. Morphological differentiation of the fossil dinosaur bone cells. *Acta Anatomica* 100:411–418.

Pawlicki, R., and M. Nowogrodzka-Zagorska. 1998. Blood vessels and red blood cells preserved in dinosaur bones. *Annals of Anatomy* 180:73–77.

Rasmussen, M., M. Jacobsson, and L. Björck. 2003. Genome-based identification and analysis of collagen-related structural motifs in bacterial and viral proteins. *The Journal of Biological Chemistry* 278:32313–32316.

San Antonio, J., M. Schweitzer, S. Jensen, R. Kalluri, M. Buckley, and J. Orgel. 2011. Dinosaur peptides suggest mechanisms of protein survival. *PLoS One* 6: e20381.

Schweitzer, M.H., and J.R. Horner. 1999. Intravascular microstructures in trabecular bone tissues of *Tyrannosaurus rex*. *Annales de Paléontologie* 85(3): 179–192.

Schweitzer, M.H., J.L. Wittmeyer, J.R. Horner, and J.K. Toporski. 2005. Soft-tissue vessels and cellular preservation in *Tyrannosaurus rex*. *Science* 307:1952–1955.

Schweitzer, M.H., J.L. Wittmeyer, and J.R. Horner. 2007a. Soft tissue and cellular preservation in vertebrate skeletal elements from the Cretaceous to the present. *Proceedings of the Royal Society B* 274:183–197.

Schweitzer, M.H., Z. Suo, R. Avci, J.M. Asara, M.A. Allen, F.T. Arce, and J.R. Horner. 2007b. Analyses of soft tissue from *Tyrannosaurus rex* suggest the presence of protein. *Science* 316:277–280.

Schweitzer, M.H., W. Zheng, C. Organ, R. Avci, Z. Sun, L. Freimark, V. Lebleu, M. Duncan, M. Heiden, J. Neveu, W. Lane, J. Cottrell, J. Horner, L. Cantley, R. Kalluri, and J. Asara. 2009. Biomolecular characterization and protein sequences of the Campanian Hadrosaur *B. Canadensis*. *Science* 324:626–631.

Schweitzer, M.H., W. Zheng, T.P. Cleland, and M. Bern. 2013. Molecular analyses of dinosaur osteocytes support the presence of endogenous molecules. *Bone* 52:414–423.

Sumper, M., and E. Bruner. 2006. Learning from diatoms: nature's tools for the production of nanostructured silica. *Advanced Functional Materials* 16:17–26.

Tesson, B, and M. Hillebrand. 2010. Dynamics of silica cell wall morphogenesis in the diatom *Cyclotella cryptica*: substructure formation and the role of microfilaments. *Journal of Structural Biology* 169:62–74.

Zylberberg, L., and M. Lauren. 2011. Analysis of fossil bone organic matrix by transmission electron microscopy. *Comptes Rendus Palevol* 10:357–366.